

Predicting Dynamic Stability of Power Grids using Graph Neural Networks

Christian Nauck, Michael Lindner, Konstantin Schürholt, Haoming Zhang, Paul Schultz, Jürgen Kurths, Ingrid Isenhardt and Frank Hellmann

Abstract—The prediction of dynamical stability of power grids becomes more important and challenging with increasing shares of renewable energy sources due to their decentralized structure, reduced inertia and volatility. We investigate the feasibility of applying graph neural networks (GNN) to predict dynamic stability of synchronisation in complex power grids using the single-node basin stability (SNBS) as a measure. To do so, we generate two synthetic datasets for grids with 20 and 100 nodes respectively and estimate SNBS using Monte-Carlo sampling. Those datasets are used to train and evaluate the performance of eight different GNN-models. All models use the full graph without simplifications as input and predict SNBS in a nodal-regression-setup. We show that SNBS can be predicted in general and the performance significantly changes using different GNN-models. Furthermore, we observe interesting transfer capabilities of our approach: GNN-models trained on smaller grids can directly be applied on larger grids without the need of retraining.

I. INTRODUCTION

THE energy transition is one of the key aspects to meet the goals of the Paris Agreement [1]. Due to decentralization, reduced inertia as well as volatility in production, integrating renewable energies remains challenging. To safely operate future power grids, the impact of unavoidable fluctuations on the synchronous operating regime has to be limited. Hence, dynamic effects have to be taken into account. Analyzing the dynamic stability of synchronisation in power grids is a complex multi-dimensional problem and many known methods rely on heavy simulations. Linear stability assessments alone, e.g. based on Lyapunov exponents, are not always applicable or sufficient. A standard in the power grid community are highly detailed simulations of individual faults. For large systems, the study of all potential individual faults is too expensive, because there are too many of them. To gain a better understanding of the type of faults that might be critical, probabilistic approaches are used. They provide an appropriate understanding and heuristics for prioritizing detailed model studies to systematically investigate the dynamic stability.

Single-node basin stability (SNBS) is such a probabilistic measure which captures highly non-linear effects and enables the analysis of large perturbations [2]. SNBS measures the probability of a grid to synchronize after applying sample-based-perturbations at individual nodes. SNBS has been applied to a variety of problems, e.g. in the engineering community for the analysis of perturbed generators in networks [3], [4] and more theoretical investigations of network properties [5]–[11]. In the non-linear dynamics and complex systems community the concept of SNBS has further been analyzed

and extended [12]–[15] to cover the type of dynamical properties that occur in realistic simulations of power grids, such as repeated perturbations, stochasticity and the influence of heterogeneity [16].

Probabilistic methods like SNBS have the advantage of assessing the robustness of locations in a network independent of specific individual faults. However, as they typically rely on Monte-Carlo sampling, they are also computationally challenging. Network theoretic methods in turn already found success at predicting dynamic properties such as SNBS [5], [6], [9], raising the potential to use network theoretic heuristics to identify key structural imprints and prioritize detailed fault simulations. For example, Schultz et al. [6] predicted SNBS using logistic regression based on network properties as input. However, the parametrization of the structure and dynamics in real power grids is highly heterogeneous, and standard network measures are not able to accommodate a wide range of node types and properties necessary for detailed, realistic dynamic models. Besides the aspect that several network measures are not well-defined for heterogeneous systems, we also do not know their relevance, because they might not translate well from homogeneous ones. Providing such information might also hinder machine learning (ML) methods from identifying new and still unknown patterns and we want to investigate how well ML methods do on their own. Hence, we hypothesize that advanced ML-methods are able to predict SNBS by using the full graph as input.

Graph Neural Networks (GNNs) are a promising approach, because they are capable of predicting certain network measures [17], [18] and can deal with full graphs as input. Therefore, we test the prediction of SNBS using GNNs. Our paper is based on a master's thesis [19] and except of this thesis, the authors are not aware of any literature using the same methods and ideas, but we introduce related work that founds on similar approaches.

Similar approaches: There are recent publications on using Graph Neural Networks in the context of power grids, but they tackle less complex problems dealing with the computation of power flows [20]–[25]. GNNs have also been used for control theory [26] and physical neural solvers have been introduced to connect GNNs with differential equations [27]. Furthermore, cascading failures were investigated in [28].

Aside from GNNs, two other publications are noteworthy to mention. Che et al. [29] recently published a paper where they show the usage of active learning and relevance vector machines to reduce the computational effort of computing SNBS by learning the boundary of stable dynamics. Further-

more, Yang et al. [30] predict the ability of power grids to synchronize after applying perturbations, but they approach the concept of dynamic stability differently. Firstly, they predict the result of single perturbations and not the statistics. Secondly, their approach is not based on providing the full graph, but they rely on common knowledge about the relation of network science and dynamic stability, e.g. by using the degree and betweenness [31] as input.

Our main contributions:

- 1) For the first time, SNBS is predicted based on the full graph instead of hand-crafted features. The focus lies on evaluating different learning methodologies based on GNNs for the sake of future research. The accuracy still needs to be improved for real world applications.
- 2) In order to train ML-models, we generate new datasets. They are based on well-known models of synthetic power grids and on Monte-Carlo simulations to analyze dynamic stability. The datasets are rich enough to challenge ML-methods, whereas still being somewhat conceptual to connect to the existing network literature. Compared to real-world power grids, synthetic power grids have a number of advantages, for example they do not have any artifacts and one can obtain more easily large datasets, which are beneficial for statistical analyses.
- 3) We also investigate transductive transfer learning capabilities by training models on small power grids and evaluating the same models on larger networks without fine-tuning.

This paper is structured as follows.: Firstly, the generation of the datasets is explained. Afterwards the background knowledge for the used ML-methods is introduced, before we present the methodology of applying our ML-models to our generated datasets. Afterwards, the results are given and discussed, before we close with a short outlook.

II. GENERATION OF THE DATASETS

To analyze the capability of predicting SNBS using ML, two synthetic datasets are generated. We start by motivating the selection of our datasets. Afterwards we briefly discuss relevant concepts from network science, before explaining the generation of synthetic power grids. We close by providing details about the dynamical simulations.

A. Objectives for datasets

High-quality datasets facilitate the application of ML-methods. Therefore, we carefully consider the following criteria for generating the datasets which mimic basic features of power grids. The datasets shall be:

- 1) somewhat homogeneous regarding their structure and dynamics to connect to network theory,
- 2) complex enough to be challenging for ML-methods,
- 3) computationally feasible using highly accurate Monte-Carlo simulations.

Firstly, homogeneity is important, because we know from previous studies, e.g. by Nitzbon et al. [9], that there are clear

relations between dynamical stability and topological properties for somewhat homogeneous grids. Hence, it is realistic, that ML-based approaches can identify relevant patterns, when using somewhat similar setups.

Secondly, we need enough complexity in our systems to justify Machine-learning models. This complexity is inherently given in the problem setup, because SNBS is a highly non-linear measure. Furthermore, we consider different network topologies.

Thirdly, we need to find a compromise between computational effort and decisive properties of the datasets, such as grid size, number of grids, low statistical errors which are determined by the number of Monte-Carlo samples and low numerical errors, which depend on the dynamical solver settings. Low statistical errors are crucial to distinguish small performance differences between ML-models later on.

Prior to generating the datasets, the influence of many parameters is investigated. We shortly motivate and explain the most important parameters for the generation of the datasets. As previously mentioned, Nitzbon et al. [9] observed interesting relations in their dataset, so we often select properties based on their investigations. Before looking at power grids in more detail, some background knowledge on graphs is needed, because power grid modeling relies on graphs.

B. Network Science: graphs

We briefly introduce theoretical background on graphs, which is also helpful to understand GNNs later on. Graphs consist of nodes (vertices) and lines (edges) connecting two nodes. The size of a graph is given by its number of nodes. To encode the topology of a graph one can use the adjacency matrix A which is defined by:

$$A_{ij} = \begin{cases} 1 & \text{if there is a line between nodes } i \text{ and } j, \\ 0 & \text{otherwise.} \end{cases} \quad (1)$$

By using the degree which is defined by the number of neighbors of a node, we can formulate the diagonal degree matrix D . Using A and D , we can compute the Graph Laplacian (L): $L = D - A$, which is a singular matrix that is a discrete analogue of the Laplace operator.

C. Power grids

The topology of the power grids is based on the tool Synthetic Networks [32]¹. This package uses a parametric growth process to generate networks. The resulting networks have properties that are suitable to observations of real-world power grid networks. We use the same parametrization as Nitzbon et al. [9]: $n_0 = 1, p = 1/5, q = 3/10, r = 1/3, s = 1/10$, where n_0 is the initial number of nodes, p, q are probabilities related to constructing new lines, s the probability of splitting an existing line and r a parameter controlling the generation of redundant paths. Furthermore, half of the nodes are producers, whereas the other half are consumers. All nodes are modeled by the swing equation [34], also referred to as a second-order

¹This tool is available on Github [33]

Kuramoto model [35], an overview is given in [36] and we use the following notation:

$$\ddot{\phi}_i = P_i - \alpha \dot{\phi}_i - \sum_j^n K_{ij} \sin(\phi_i - \phi_j), \quad (2)$$

where $\phi, \dot{\phi}, \ddot{\phi}$ denotes the voltage angle and its time derivatives. We use the following parametrization: $P_i \in \{-1, 1\}$ the injected power, $\alpha = 0.1$ the damping coefficient, K is the coupling matrix based on the adjacency matrix which encodes the graph and we use uniform coupling $K_{ij} = 9A_{ij}$. The values for the injected power and the damping coefficient are the same as in [9], however we use a larger coupling (9.0 instead of 6.0) to increase the overall stability of synchronisation in the power grids, which is more realistic, and to obtain a clear bi-modal shape of the SNBS-distribution for a better balance for training ML-methods. We are interested in deviations from the nominal frequency (e.g. 50Hz in Europe), and thus will work in frequency deviations throughout the paper. The desired state is thus $\dot{\phi}_i = 0$ at all nodes.

D. Dataset properties

We study the resilience of power grids operating in their synchronous state to (large) perturbations at individual nodes. The single-node basin stability of a node is quantified as the probability that the systems returns to its synchronized state after such a network-local perturbation. Since the perturbations are drawn independently at random, SNBS is the outcome of a Bernoulli experiment [2].

To estimate SNBS for every node in a graph, samples of $N = 10,000$ perturbations per node are constructed by sampling a phase and frequency deviation from a uniform distribution with $(\phi, \dot{\phi}) \in [-\pi, \pi] \times [-15, 15]$ and adding them to the synchronized state. Each such single-node perturbation serves as an initial condition of a dynamic simulation of our power grid model, cf. Equation (2). At $t = 500$ the integration is terminated and the outcome of the Bernoulli trial is derived from the final state. A simulation outcome is referred to as *stable* if at all nodes $\dot{\phi}_i < 0.1$. Otherwise it is referred to as *unstable*. Two exemplary trajectories are shown in fig. 1.

The classification threshold of 0.1 is chosen accounting for minor deviations due to numerical noise and slow convergence rates within a finite time-horizon. The authors are not aware of any other attractors of the Kuramoto system within that threshold. Hence, it may be assumed that every trajectory labeled as stable in that way will indeed converge to the synchronous state for $t \rightarrow \infty$. On the other hand, trajectories who are classified as unstable may converge to many different kinds of attractors [37], [38]. However, we occasionally observed so-called *long transient states* at specific nodes, which do eventually converge to the synchronous state but fail to do so before $t = 500$. While of theoretical interest, we do not expect their asymptotic behaviour to play any role in real world applications and thus we are satisfied with classifying them as unstable.

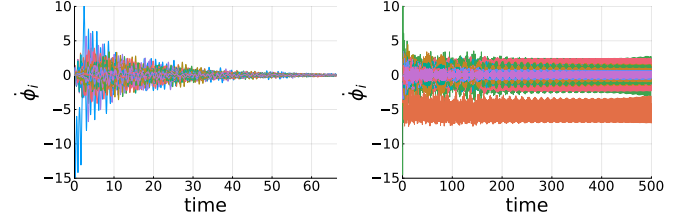


Fig. 1. Exemplary trajectories of applying single-node perturbations to a grid of 100 nodes. A stable state is reached on the left and an unstable state on the right after applying different single-node perturbations at different nodes. Different colors represent the trajectories at different nodes.

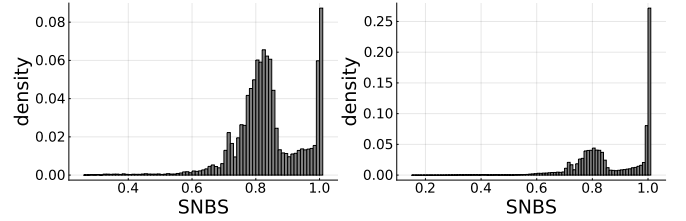


Fig. 2. Histogram showing the distribution of SNBS for the datasets with 20 nodes (left) and 100 nodes (right). The distributions are normalized so that bin heights sum to 1.

A 95% confidence interval for the estimated SNBS values may be determined via the normal distribution approximation of the Bernoulli experiment as [39]:

$$1.96 \sqrt{\frac{p(1-p)}{N}} < 0.01, \quad (3)$$

where the inequality is obtained by setting $p = 0.5$ and $N = 10,000$.

The distributions of SNBS for both datasets are given in fig. 2. We refer to the dataset consisting of grids of 20 nodes per grid as *dataset20*, and to the dataset consisting of grids of size 100 nodes as *dataset100*. For both cases, there is a bi-modal distribution of SNBS over the whole data set, which facilitates ML-models to learn the distinction between those modes. The peak at 1.0 indicates a large amount of nodes where no perturbation has an adverse effect on the synchronisation. The second peak can be interpreted in a way that many nodes are somewhat resistant to perturbations and the grid stays synchronised in about 80% when applying perturbations at the particular nodes. In case of *dataset20* the mean value of SNBS is 0.84 and for *dataset100* nodes it is 0.87. In both datasets, the number of unstable outcomes is low, which is a property we expect to hold for real power grids as well.

III. GRAPH NEURAL NETWORKS

This section briefly introduces Graph Neural Networks (GNNs). We begin with a general framework for GNNs and subsequently summarize the recent development of GNNs. Graph Neural Networks are a class of Artificial Neural Networks (ANN) designed to learn relationships of graph-structured data. Just as ANNs they have internal weights,

which can be fitted in order to adapt their behavior to the given task. In the case of supervised learning these weights are adjusted such that the error between the estimated output and the labeled output for given input data is minimized. As inputs GNNs use the graph structure and potentially node features. Their output can either be global graph attributes, attributes of sub-graphs, or local node properties. Different types of GNNs have been introduced, some of which are detailed below. In [40], the authors introduce a *design space* for GNNs as a common framework to facilitate understanding and comparison of the different methods. In their design space, GNNs consist of pre-processing, message-passing and post-processing layers. GNN architectures vary in layer number and connectivity, as well as the intra-layer design of the message-passing layers. [40] view message-passing layers as combinations of (i) message computation and (ii) aggregation. First, a message function computes a message for each node from its current state. Secondly, the messages are aggregated over the neighborhood to a new node state. Both message computation and aggregation can be realized in different ways. Common ML-methods such as *batch normalization* [41] or *dropout* [42] can be added to stabilize training. The application of non-linear activation functions enables GNNs to learn non-linear relations in the graph data. In this work we focus on convolutional GNNs and in particular on those employing spatial-based graph convolutions, because they can be applied to varying topologies, as we have in our datasets.

Graph convolutions are based on the concept of the Graph Fourier transform, a generalization of the classical Fourier transform (FT), which enables the remarkable success of Convolutional Neural Networks (CNN) in image recognition. Unlike the classical FT, which uses exponential shifts the Graph FT corresponds to an expansion of the function on the graph in terms of the eigenvectors of the graph Laplacian L . Such an expansion may in turn be multiplied with a function of the graphs eigenvalues, a so-called spectral filter. While it is possible to learn spectral filters from training data, they lack many of the nice properties of the convolution kernels used in CNNs: they are not localized in node space, computing the eigenbasis is expensive and trained models can not be evaluated on different graphs, since each graph has a unique spectrum.

An important insight of [43] was that graph spectral filters can be approximated by polynomials of the graphs' adjacency matrix A , thus achieving a localization of the filter in the (k -th order) neighborhoods of the nodes. Subsequently, in their seminal paper Kipf and Welling [44] realized that it suffices to consider only the linear term of the polynomial expansion, corresponding to a simple multiplication of the node features with the (renormalized) adjacency matrix. They arrived at a computationally efficient and powerful layer architecture that relies only on local information and generalizes well to different graphs. Several GNN models that we investigate in this paper were derived from their so-called Graph Convolutional Layer (GCN):

$$H = \sigma(\bar{A}X\Theta), \quad (4)$$

where H denotes the output of a layer, σ is the activation function, X are the input features, Θ is a matrix containing the learnable weights and \bar{A} is the renormalized adjacency matrix, given by $\bar{A} = \tilde{D}^{-\frac{1}{2}} \tilde{A} \tilde{D}^{-\frac{1}{2}}$. Further $\tilde{A} = A + I$, where I is the identity matrix, denotes an adjacency matrix with added self-loops and the diagonal degree matrix \tilde{D} is determined by: $\tilde{D}_{ii} = \sum_j \tilde{A}_{ij}$. In the design space of [40], $X\Theta$ manifest the message computation, while \bar{A} realizes the aggregation. By consecutively applying multiple GCN-layers, not only direct neighbors are taken into account, but also neighbors at further distance.

Instead of stacking multiple GCN-layers, Wu et al. [45] removed the activation functions, combined all weight matrices into one and computed \tilde{A}^i to obtain:

$$H = \text{softmax}(\bar{A}^i X \Theta). \quad (5)$$

This layer founds on their assumption that the nonlinearity between GCN layers is not crucial and may be omitted in order to reduce computational effort. We refer to this layer as Simple-Graph-Convolution (SG).

Du et al. [46] used multiple exponents i of \tilde{A} within one layer according to the following scheme:

$$H = \sum_{z=0}^Z D^{-\frac{1}{2}} A^z D^{-\frac{1}{2}} X \Theta_z. \quad (6)$$

This layer type is called Topology Adaptive Graph Convolution (TAG), which refers to its ability of considering different topologies. However, this is the case for all methods that are introduced in this paper. This architecture provides an extension to GCNs by incorporating information about higher order neighborhoods within one layer.

Auto-Regressive Moving Average (ARMA) neural network layers by Bianchi et al. [47] are far-reaching generalizations of GCN layers. They are derived from a rational expansion of the spectral filter instead of a polynomial expansion. A complete ARMA-layer consists itself of multiple Graph Convolutional Skip (GCS) layers:

$$\bar{X}^{(t+1)} = \sigma(\tilde{L}X^{(t)}W^{(t)} + XV^{(t)}), \quad (7)$$

where W and V are matrices of trainable parameters. There are two important distinctions from the GCN layers: the aggregation in the first term uses normalized Laplacian $\tilde{L} = I - D^{-\frac{1}{2}}AD^{-\frac{1}{2}}$, instead of \tilde{A} . Additionally, the connectivity of the message-passing layers is augmented with a skip connection, implemented in the second term. It recursively re-inserts the initial node features X from the first layer and thus enables stacking a large number of GCS layers, whereas preventing the loss of the initial information due to Laplacian smoothing. In order to reduce the computational effort and to reduce overfitting, the weights among different GCS layers are shared: $W^{(t)} = W$ and $V_{(t)} = V$, except for the first layer where $W^{(1)} \neq W$.

To increase their expressive power multiple ARMA layers may be combined in a parallel stack:

$$\bar{X} = \frac{1}{K} \sum_{k=1}^K \bar{X}_k^{(T)}, \quad (8)$$

TABLE I
PROPERTIES OF DATASETS

name	number of grids	number of nodes per grid	SNBS
dataset20	1000	20	0.8398
train	800	20	0.8407
test	200	20	0.8365
dataset100	1000	100	0.8737
train	800	100	0.8730
test	200	100	0.8768

where $\bar{X}_k^{(T)}$ is the output of the last GCS layer in the k -th ARMA layer. ARMA filters with their recursive and distributed formulation, are efficient to train and capable of learning complex information. All of the layers described above are used in the models introduced in the next section.

IV. PREDICTION OF SNBS USING GRAPH NEURAL NETWORKS

To predict SNBS of all nodes, we use a node-regression setup, by providing the weighted adjacency matrix of the graph and the injected power per node P_i as inputs. In order to test the performance of our models on unseen data, we split the datasets into training and testing sets. The shift between them is marginal as can be seen in Table I.

A. Setup of our GNN-models

Based on the introduced GNN layers, eight GNN-models are analyzed to evaluate the performance of different architectures. GNNs are capable of reading in the full graph without any simplifications. We also tried to use CNNs which are well known from image analysis. In case of CNNs, the graph information is provided by using a modified version of the adjacency matrix as input, but the setup had several limitations in comparison to the GNNs. The application of CNNs is shown in Appendix E. In Table II the GNN-models are briefly introduced. All models use one type of graph convolutional layer, but may use several numbers of them and all have one linear and one sigmoid layer at the end. Additionally, dropout is used in several cases, cf. Appendix B. We did not do a systematic investigation of hyperparameters such as number of layers and their properties, but focused on identifying relevant factors to enable training.

B. Training setup

For all models the same parameters are used and the training consists of 500 epochs. To enable reproducibility, the seeds are set before training and can be found in the published source code ². The training is based on the software Pytorch [48] and for the graph handling and graph convolutional layers the additional library PyTorch Geometric [49] is used. For the training of the models, CPUs are used and depending on the model training takes between 20 minutes and 50 minutes on either Haswell or Broadwell architecture without parallelization. The detailed training parameters, e.g. batch

TABLE II
PROPERTIES OF MODELS. NUMBER OF PARAMETERS DENOTES THE NUMBER OF LEARNABLE WEIGHTS OF THE MODEL.

name	type of convolution	number of layers	number of parameters	maximum number of hops
ArmaNet1	ARMA	1	38	4
ArmaNet2*	ARMA	2	1050	8
GCNNet1	GCN	2	15	2
GCNNet2	GCN	3	107	3
GCNNet3*	GCN	3	149	3
SGNet1	SG	1	4	2
SGNet2	SG	2	15	4
TAGNet1	TAG	2	39	6

* There is a batch normalization between first and second layer.

sizes and additional information on the computational effort are given in Appendix C. As loss function we use the mean squared error ³.

V. RESULTS

To evaluate the performance of different models, the R^2 score, which may also be known as coefficient of determination and a self-defined discretized accuracy is used. The score R^2 is computed by:

$$R^2 = 1 - \frac{mse(y, t)}{mse(t_{mean}, t)}, \quad (9)$$

where mse denotes the mean squared error, y the output of the model, t the target value and t_{mean} the mean of all considered targets of the test dataset. The standard measure of performance is R^2 , which captures the mean square error relative to a null model that predicts the mean of the test-dataset for all points. A constant model that always predicts t_{mean} , disregarding the input features, would get a score of $R^2 = 0.0$. The R^2 -score is used to measure the portion of explained variance in a dataset. To further simplify interpretation, we rephrase the evaluation as a classification problem.

The outputs are categorized as true or false by using a threshold and we compute the accuracy as:

$$\text{discretized accuracy} = 1 - \frac{\text{true positives} + \text{true negatives}}{\text{number of samples}}. \quad (10)$$

We refer to this self-defined accuracy as *discretized accuracy*. Predictions are considered to be correct, if the predicted output y is within a certain threshold to the target value t : $y - t < \text{threshold}$. We set this threshold to 0.1, because this is small enough to differentiate between the modes in the distributions (see fig. 2). Furthermore, a total deviation of the prediction and true output of 0.1 should be efficient for most applications. The discretized accuracy depends on the distribution of SNBS, so it can not be used for comparison across different datasets, but has to be compared to the null model of the corresponding dataset.

Since there is no previous work that can be easily compared to our methods, we introduce a simple baseline model. This baseline model always predicts the average value of the testing

²Information regarding the full source code is given in Appendix A

³corresponds to MSELoss in Pytorch

TABLE III
RESULTS REPRESENTED BY R^2 SCORE IN %

model	dataset20	dataset100	tr20ev100
ArmaNet1	18.8	15.4	3.60
ArmaNet2	39.5	45.4	23.7
GCNNet1	8.10	5.98	-3.22
GCNNet2	24.3	22.1	13.2
GCNNet3	9.02	6.71	-0.67
SGNet1	7.12	3.98	-9.15
SGNet2	13.5	13.0	1.67
TAGNet1	29.1	28.8	13.7

For dataset20 and dataset100, the models are both trained on their training and evaluated on their test sections. To evaluate the transfer learning capabilities, we use the term *tr20ev100* meaning that the model is trained on the dataset20, but evaluated on the dataset100.

TABLE IV
RESULTS REPRESENTED BY DISCRETIZED ACCURACY IN %

model	dataset20	dataset100	tr20ev100
ArmaNet1	76.5	65.1	56.0
ArmaNet2	80.5	85.0	65.9
GCNNet1	69.5	66.6	47.8
GCNNet2	79.8	67.5	59.8
GCNNet3	71.6	63.7	49.5
SGNet1	67.9	67.8	46.0
SGNet2	70.5	65.9	48.7
TAGNet1	78.8	69.6	56.1

For dataset20 and dataset100, the models are both trained on their training and evaluated on their test sections. To evaluate the transfer learning capabilities, we use the term *tr20ev100* meaning that the model is trained on the dataset20, but evaluated on the dataset100.

set. By design, this results in $R^2 = 0$, and achieves a discretized accuracy of 67.1 % on dataset20 and of 40.9% on dataset100. The differences in discretized accuracy are rooted in the different distributions of the two datasets (cf. fig. 2).

We use an averaged performance to reduce the impact of the initialization effects. Out of 5 different initializations per training setup, only the best three are considered to compute an averaged performance. The average R^2 -performance is given in Table III and for the discretized accuracy in Table IV. The best values are in bold. The training progress of the best model is shown in fig. 3.

Furthermore, we investigate whether the features learned by GNNs generalize to grids of different sizes. As datasets of large grids are costly to create, successful pre-training on smaller grids with subsequent application on larger grids would be a valuable strategy. To evaluate the transfer learning capabilities, we train GNN-models on the small dataset of grids with 20 nodes and evaluate without fine-tuning on the dataset with large grids of 100 nodes. As performance of the transductive transfer learning, we report the R^2 and accuracy on the large target dataset using the term *tr20ev100* (trained on dataset20, evaluated on dataset100).

The results show that the prediction of SNBS using GNNs is feasible and different models have a large impact. We did not perform a detailed hyperparameter study of different GNN-models, so conclusions about their performance are tentative for now. Next, we shortly summarize our observations. The results indicate that increasing the complexity of the model can be beneficial, as the model ArmaNet2 with the largest

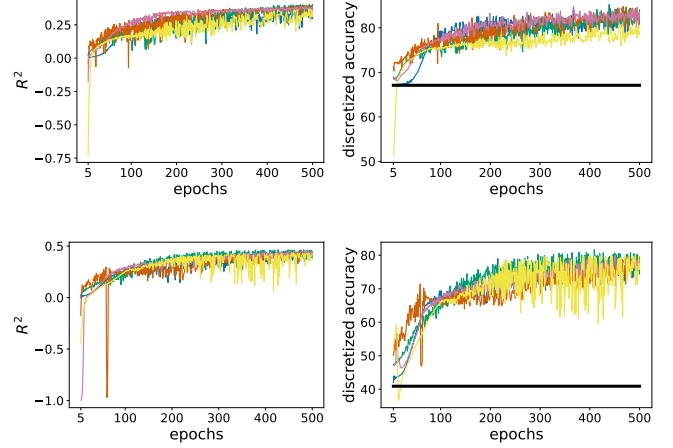


Fig. 3. Training results for ArmaNet2 and dataset20 at the top and dataset100 at the bottom. The R^2 -score is shown on the left and the test discretized accuracy on the right. Different colors show different initializations and the horizontal line for the discretized accuracy is based on a toy model that always predicts *SNBS*. The evaluation is purely based on the test dataset.

amount of parameters (1050) performs best. However, increasing the complexity is not always helpful. GCNNet3 for example performs worse than GCN2, even though having more learnable parameters (149 instead of 107). The meaning of the type of convolution is underlined by considering TAGNet1 and ArmaNet1, because TAGNet1 outperforms ArmaNet1 with only slightly more parameters than ArmaNet1. Figure 4 shows the relation of the complexity and performance based on dataset100. The complexity is firstly represented by the number of learnable parameters on a logarithmic scale and secondly by the maximum number of possible hops. By hops we mean the order of neighbors that are taken into account. For example, one hop means that only direct neighbors are considered, whereas two means that nodes are considered which are not directly connected, but via one direct neighbor.

Without conducting ablation studies, we can only guess reasons for the superiority of ArmaNet2 and mainly think of two reasons. It could be firstly, the largest number of parameters, and secondly the most complex architecture including skip layers which enables a deep setup to consider neighbors of higher degrees. By having four GCS-layers in both ArmaNet-layers, a relatively large region can be considered in case of ArmaNet2. TAGNet1 also performs well and this model can evaluate neighbors of 6th-order, by having two layers and three hops per layer. The benefit of ArmaNet2 can be emphasized by investigating *tr20ev100*, because ArmaNet2 outperforms all other models on dataset100, even if it is purely trained on dataset20. Hence, the models ArmaNet2 results in the most robust setup.

To further evaluate the performance of the investigated models, we analyze the distribution of the output of selected models in fig. 5. Therefor, we only consider the output based on the best seed per model using R^2 as a criterion. The output of all models is restricted to somewhat large values and neither low nor very high values of SNBS can be predicted. The small amount of nodes with low SNBS in the dataset might

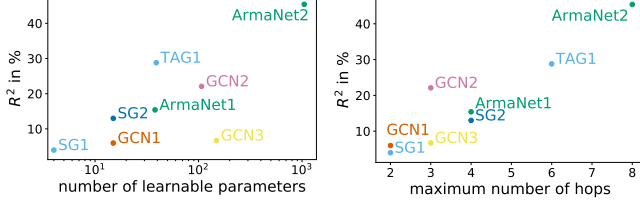


Fig. 4. Relation of performance and the complexity of models represented by the number of learnable parameters on the left and the number of maximum hops on the right. The plotted results are based on dataset100.

explain the absence of low output values. In case of large output values, it is remarkable and a bit surprising that none of the models predicts the abundance of completely stable outcomes. This behaviour limits the applicability to real world problems. The limitation of all models also becomes clear when comparing the results to the distributions introduced in fig. 2. Since the shifts⁴ within the datasets are small, we can compare the output distributions to the distributions of the entire datasets, even though fig. 5 only considers the test section.

The distributions of the output (fig. 5) also indicate performance differences between the models. We clearly see that GCN1, having a relatively low performance, has a very limited range of output values and all values are around the mean of the dataset. ArmaNet1 already has a wider range, whereas ArmaNet2 has the largest range. Besides the range, the shape of the distribution and modalities of the predictions are also telling, e.g. we find an indication for a bimodal distribution in case of TAGNet1. All in all, the superiority of ArmaNet2 and TAGNet1 becomes visible. However, even for those models the output is still limited to values that are larger than 0.6 and there is only a small amount of predictions of high stability (SNBS \approx 1).

To visually analyze the models, we plot the predicted output vs. SNBS in heat maps in fig. 6. Perfect predictions would be on the diagonal only, similarly to $R^2 = 1$. On the contrary to R^2 shown in table III, we can find some reasons for the performance differences. We see that ArmaNet2 and TAGNet1 can distinguish between nodes with SNBS \approx 1 and nodes with lower SNBS. Other models, such as GCN1, have large regions on the off-diagonal, resulting in a lower performance.

VI. CONCLUSION AND OUTLOOK

The key result of this paper is a novel approach of estimating SNBS via GNNs. We have demonstrated its potentials and have paved the way for further investigations. We show the necessity to use well-adapted architectures for this problem, since generic CNNs are not able to achieve comparable results even with more parameters (cf. Appendix E).

The strongest limitation of the presented results are probably the assumptions for generating the datasets which matches several properties of real power grids, but it also simplifies some aspects, e.g. missing heterogeneity of nodes (power input) and

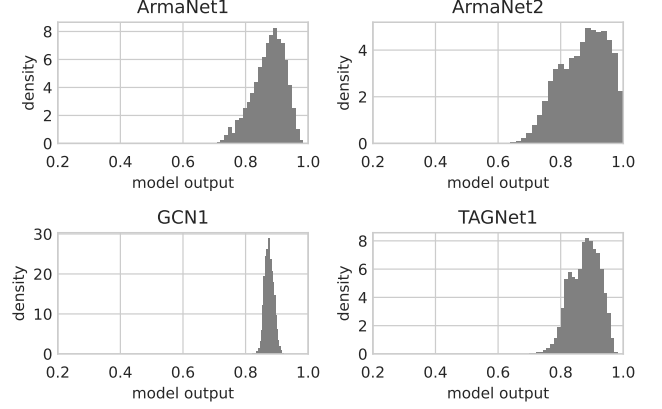


Fig. 5. Histograms showing density of predicted outputs for different models and dataset100 and the best seed per model.

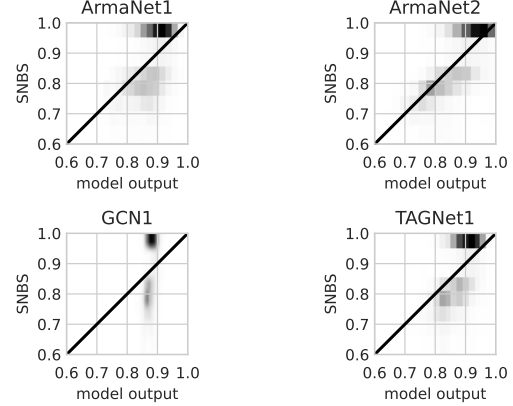


Fig. 6. Heat maps of comparing models using the best seed for each of them and considering the predicted output vs. SNBS and investigating dataset100. The diagonal represents a potential perfect model ($R^2 = 1$).

lines (coupling constant). However, the accuracy can still be increased before moving to more realistic setups, because the performance is still too low for real applications. We provide several ideas for improvements in the next paragraphs.

Since we see substantially improved performance for models with larger number of parameters testing more complex models seems very promising. More complex models might identify other relevant structures of networks to predict SNBS more accurately, there is no suggestion that the performance is already saturating. As a first step, one could conduct a hyperparameter study to improve the investigated models.

In further steps, one could introduce new models to increase the performance. Firstly, new layers could be designed that specifically aim to predict SNBS and deal with power grids. Secondly, hybrid approaches might be used that incorporate knowledge about known structures, e.g. network motifs that can hardly be recognized by GNNs. Generally it is clear from our results that more complex architectures are promising for this task, even if it remains unclear exactly what direction the complexity increase should point towards.

Another key for improvement are the datasets. The used datasets are relatively small, so increasing the size of the

⁴A dataset shift means, that training and testing datasets are different.

TABLE V
SOFTWARE PACKAGES FOR ML

package	version	package	version
Cuda	10.2	torch-cluster	1.5.9
h5py	2.10.0	torch-geometric	1.7.0
numpy	1.19.2	torch-scatter	2.0.6
pandas	1.2.4	torch-sparse	0.6.9
python	3.8.5	torch-spline-conv	1.2.1
pytorch	1.7.1	torchvision	0.8.2

datasets might be an important step for training more complex models. To solve the issue of the limited range of outputs and the observation that the model outputs are around the mean of the datasets, balancing or weighting of samples might help.

Remarkably, we successfully showed that GNNs can generalize across different sizes of power grids. Another avenue for future research is to train models based on different sizes to start with. It is feasible that the overall performance can be increased when actually training the models on multiple datasets. The capability of training models on smaller grids and applying them on larger grids can become crucial for real-world applications to reduce the computational effort of generating datasets and also the training the models.

APPENDIX A SOURCE CODE

The full source code including the dataset is available at <https://zenodo.org/record/5148085>. Furthermore, the scripts are also given at Github https://github.com/PIK-ICoNe/paper-companion_predicting-snbs-using-gnn. The code for the computation of SNBS is written in Julia [50] and the dynamic simulations rely on the package DifferentialEquations.jl [51]. For simulating more realistic power grids in future work we recommend the additional use of NetworkDynamics.jl [52] and PowerDynamics.jl [53]. Software packages used for ML-applications are listed in Table V:

APPENDIX B MODEL DETAILS

In this section details about the used models are provided, whereby NIC denotes the number of input channels, NOC the number of output channels, NOH the number of hops per layer (for TAGConv and SGConv) and ReLU the rectified linear unit activation function. Recall that we only have one node feature as input and hence our most common choice for NIC is 1.

1) *ArmaNet1*:

- Arma-Convolution (NIC = 1, NOC = 1, num-stacks = 3, num-layers = 4, ReLU activation, weights are not shared between layers),
- fully connected layer and sigmoid output layer.

2) *ArmaNet2*:

- Arma-Convolution (NIC = 1, NOC = 16, num-stacks = 3, num-layers = 4, dropout = 0.25, ReLU activation, weights are shared between layers),
- Batch normalization, ReLU and dropout,

- Arma-Convolution (NIC = 16, NOC = 1, num-stacks = 3, num-layers = 4, dropout = 0.25, no activation function, weights are shared between layers),
- fully connected layer and sigmoid output layer.

3) *GCNNet1*:

- GCN-convolution (NIC = 1, NOC = 4),
- ReLU and dropout,
- GCN-convolution (NIC = 4, NOC = 1),
- fully connected layer and sigmoid output layer.

4) *GCNNet2*:

- GCN-convolution (NIC = 1, NOC = 16),
- ReLU and dropout,
- GCN-convolution (NIC = 16, NOC = 4),
- ReLU,
- GCN-convolution (NIC = 4, NOC = 1),
- fully connected layer and sigmoid output layer.

5) *GCNNet3*:

- GCN-convolution (NIC = 1, NOC = 16),
- batch normalization, ReLU and dropout,
- GCN-convolution (NIC = 16, NOC = 4),
- batch normalization, ReLU
- GCN-convolution (NIC = 4, NOC = 1),
- fully connected layer and sigmoid output layer.

6) *SGNet1* :

- SG-Convolution (NIC = 1, NOC = 1, NOH = 2),
- ReLU, fully connected layer and sigmoid output layer.

7) *SGNet2*:

- SG-Convolution (NIC = 1, NOC = 4, NOH = 2),
- ReLU, dropout,
- SG-Convolution (NIC = 4, NOC = 1, NOH = 2),
- fully connected layer and sigmoid output layer.

8) *SGNet3*:

- SG-Convolution (NIC = 1, NOC = 16, NOH = 2),
- ReLU, dropout,
- SG-Convolution (NIC = 16, NOC = 4, NOH = 2),
- ReLU,
- SG-Convolution (NIC = 4, NOC = 1, NOH = 2),
- fully connected layer and sigmoid output layer.

9) *TAGNet1*:

- TAG-Convolution (NIC = 1, NOC = 4, NOH = 3),
- ReLU, dropout,
- TAG-Convolution (NIC = 4, NOC = 1, NOH = 3),
- fully connected layer and sigmoid output layer.

APPENDIX C TRAINING DETAILS

The used training parameters can be found in Table VI. The scripts include seeds for

`torch, cuda and numpy.random,`

even though cuda may not be used. The computation times are given in Table VII. The times should only be a rough estimation.

TABLE VI
PARAMETERS FOR ML

parameter	property	parameter	property
training batchsize	100	test batchsize	200
trainig set index	1-800	test set index	801-1000
train set shuffle	true	test set shuffle	false
optimizer	SGD	learning rate	0.3
momentum	0.9	weight decay	1e-9
criterion	MSELoss	threshold for discretized accuracy	0.1

TABLE VII
TRAINING TIME WHEN USING GNNs

dataset	model	architecture	training time [hh:mm]	ram usage in cores
dataset20	ArmaNet1	Haswell	0:25	1
dataset20	ArmaNet2	Haswell	0:26	1
dataset20	TAGNet1	Broadwell	0:24	1
dataset20	SGNet1	Haswell	0:21	1
dataset20	SGNet2	Haswell	0:22	1
dataset20	GCNNNet1	Broadwell	0:23	1
dataset20	GCNNNet2	Broadwell	0:24	1
dataset20	GCNNNet3	Haswell	0:24	1
dataset100	ArmaNet1	Haswell	0:28	1
dataset100	ArmaNet2	Haswell	0:47	1
dataset100	TAGNet1	Haswell	0:30	1
dataset100	SGNet1	Haswell	0:28	1
dataset100	SGNet2	Haswell	0:28	1
dataset100	GCNNNet1	Haswell	0:30	1
dataset100	GCNNNet2	Haswell	0:29	1
dataset100	GCNNNet3	Haswell	0:31	1

APPENDIX D

ADDITIONAL RESULTS USING GRAPH NEURAL NETWORKS

In this section, we only briefly show more figures. The performances are already given in Tables III and IV. The distribution of the predicted outputs and heat maps for the remaining models applied to dataset100 are shown in fig. 7. None of those models are able to predict any completely stable nodes.

For dataset20 the output distributions and heat maps are shown in figs. 8 and 9. For dataset20 the distinction between nodes of $SNBS \approx 1$ and nodes that are less stable is more challenging, because there are less nodes of $SNBS \approx 1$ in the dataset. Comparing models based on the heat maps and distributions only is more challenging for dataset20, which is most likely because of the different distributions of the dataset and less stable outcomes. The relation between performance and model complexity as measured by the number of trainable parameters and the number of total hops respectively is shown in fig. 10.

APPENDIX E

CONVOLUTIONAL NEURAL NETWORKS

Convolutional Neural Networks (CNNs) are one of the key technologies for image recognition. Convolutional layers aggregate spatial information of nodes (pixels) by evaluating the relations of pixels and their neighbors. We investigate if slightly modified CNNs can be used to analyze graphs. When analyzing images the input for a CNN is provided as matrices

where each pixel is described by a floating point number. Similarly, we provide different input matrices derived from the graphs' adjacency matrix which encode the topology of the graphs. To ensure comparability of different graphs and to break symmetries, the nodes are ordered using the current-flow betweenness [54].

A. Our approach of applying CNNs

Besides the adjacency matrix, nodal information needs to be provided to the model. When using colored images, the different RGB colors are provided in multiple channels to the CNN. In our case, at each node the power injection P (and extraction respectively) is provided in two different ways:

- 1) Firstly, an additional row is added to the graph Laplacian L , leading to an input of $1 \times (n + 1) \times n$ per sample.⁵
- 2) Secondly, another channel, containing information of P in a matrix of size $\mathbb{R}^{n \times n}$ is added, where all non-diagonal elements are zero and the diagonal consists of P_i . So the input has the following dimension: $(2 \times n \times n)$.

We refer to the first approach as 1C and to the second as 2C.

To analyze the performance using CNNs, three residual nets are compared, which consist of 18, 34 and 50 layers. All three models are only slightly modified with respect to the original models [55] to meet the requirements of the dimension of the input and output. We do not use pre-trained models, because that did not help in our investigated cases.

B. Results of training CNNs

The same training parameters are used as introduced in Table VI. The training effort when using 100 epochs is given in table VIII and the results are shown in table IX. The results are represented by R^2 score on the left and discretized accuracy on the right.

In comparison to GNNs, the training is less robust with large fluctuations during training and overfitting may occur quickly. For example the results are plotted for ResNet34 (2C) for dataset100 in fig. 13. The results for 1C or dataset20 and other models look very similar. All CNNs achieve comparable performance and outperform low performing GNN-models such as ArmaNet1, GCNNNet1, GCNNNet3, SSGNet1 and SGNet2. However, the models cannot deal with flexible grid sizes. Furthermore, the best GNN-models outperform CNNs by far, so using CNNs seems to be less promising. The input formats (1C and 2C) do not have a large impact.

ACKNOWLEDGMENT

The authors would like to thank the Chair of Information Management in Mechanical Engineering of RWTH Aachen University for computational resources. Christian Nauck would like to thank the German Federal Environmental Foundation (DBU) for funding his PhD scholarship and Professor Raisch from Technical University Berlin for supervising his PhD. Michael Lindner greatly acknowledges support by the Berlin International Graduate School in Model and Simulation

⁵First factor shows the number of input channels

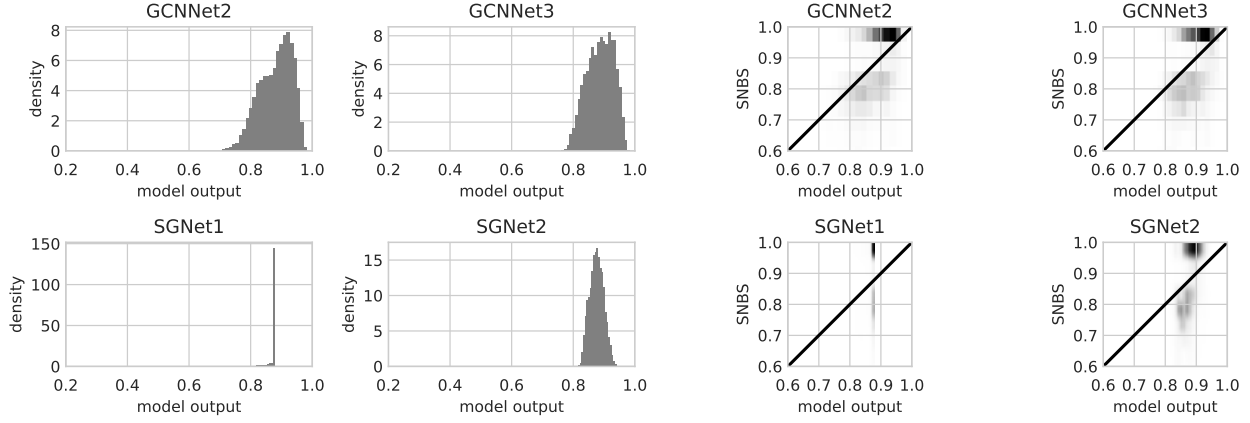


Fig. 7. Remaining results for dataset100 using the best seed per model. On the left: Histograms showing density of predicted outputs. On the right: Heat maps of predicted output vs. SNBS. The diagonal represents a potential perfect model ($R^2 = 1$).

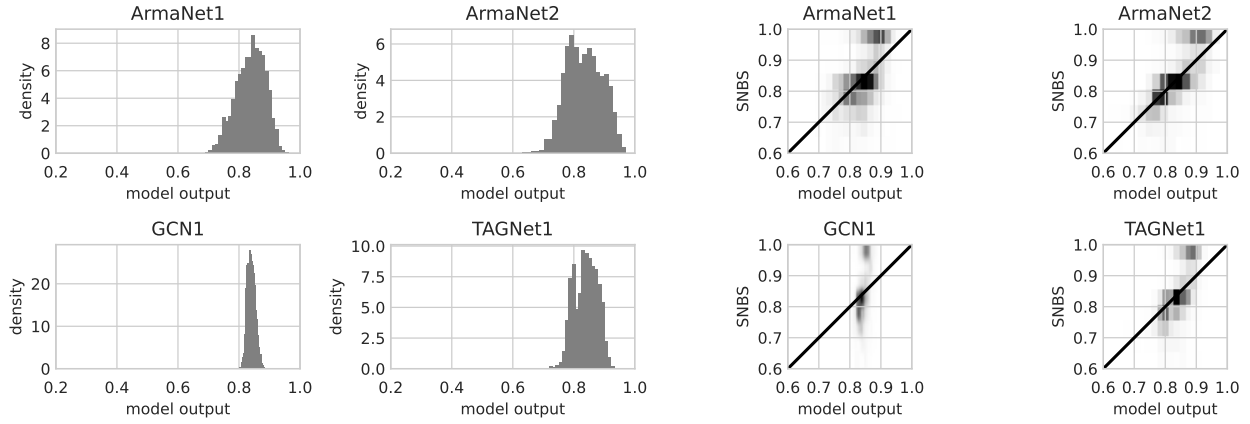


Fig. 8. Results of several models using best seed per model for dataset20. Left: Histograms showing density of predicted outputs, corresponds to fig. 5. Right: Heat maps of predicted output vs. SNBS, corresponds to fig. 6.

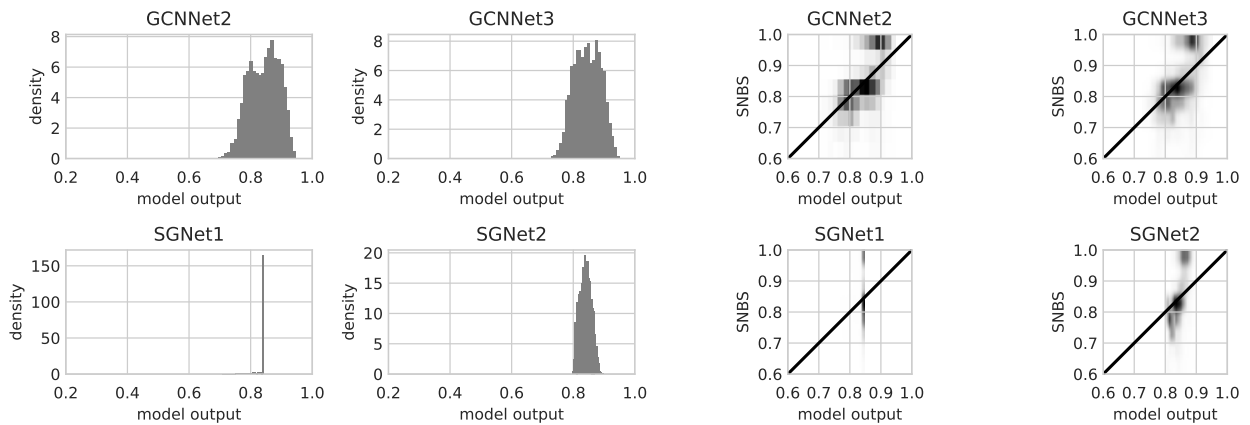


Fig. 9. Results of remaining model using best seed per model for dataset20. Left: Histograms showing density of predicted outputs. Right: Heat maps of predicted output vs. SNBS. This figure corresponds to fig. 7.

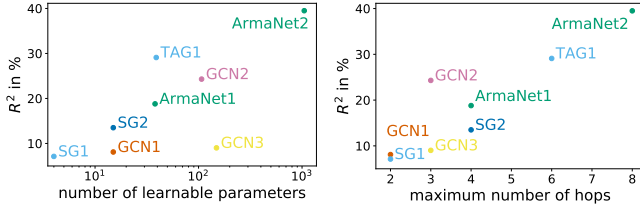


Fig. 10. Relation of performance as measured by the R^2 and the complexity of models represented by the number of learnable parameters on the left and the total number of hops on the right. Results are based on dataset20.

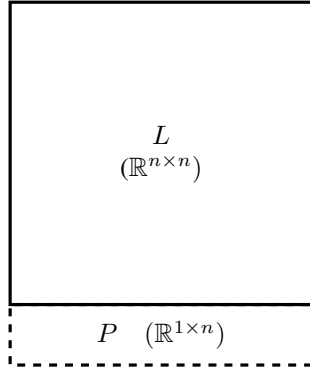


Fig. 11. Adding P in another row, Input of size: $1 \times (n + 1) \times n$. We refer to this approach as 1C.

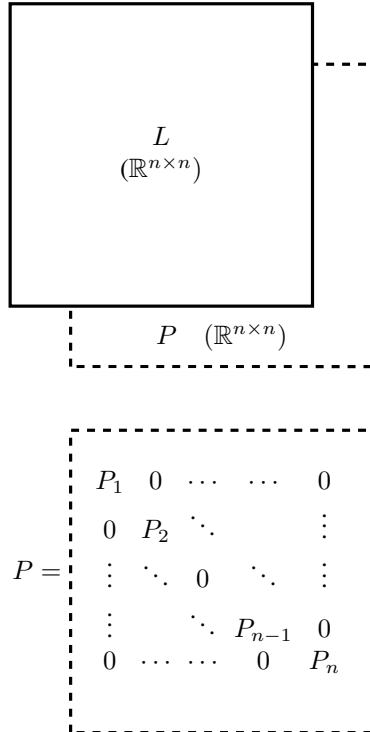


Fig. 12. Concatenating another channel P . We refer to this approach as 2C.

TABLE VIII
TRAINING TIME FOR CNNs AND 100 EPOCHS

dataset	model	architecture	training time [hh:mm]	ram usage in cores
dataset20	ResNet18	Haswell	0:40	1
dataset20	ResNet34	Haswell	4:00	1
dataset20	ResNet50	Broadwell	4:00	1
dataset100	ResNet18	Haswell	2:45	3
dataset100	ResNet34	Haswell	5:34	4
dataset100	ResNet50	Haswell	7:25	5

TABLE IX
RESULTS WHEN USING CNNs

model	R^2 score in %				discretized accuracy in %			
	dataset20 1C	dataset20 2C	dataset100 1C	dataset100 2C	dataset20 1C	dataset20 2C	dataset100 1C	dataset100 2C
ResNet18	16.1	14.1	20.5	20.2	78.4	78.2	69.3	69.3
ResNet34	17.4	16.6	21.2	20.6	79.0	78.6	69.2	69.2
ResNet50	16.6	15.2	20.7	20.7	78.2	78.1	69.3	69.3

based Research (BIMoS) of TU Berlin. All authors gratefully acknowledge the European Regional Development Fund (ERDF), the German Federal Ministry of Education and Research, and the Land Brandenburg for supporting this project by providing resources on the high-performance computer system at the Potsdam Institute for Climate Impact Research. This work was funded by the Deutsche Forschungsgemeinschaft (DFG, German Research Foundation) – KU 837/39-1 / RA 516/13-1.

REFERENCES

- [1] United Nations, *PARIS AGREEMENT*. Paris: 21st Conference of the Parties, 2015. [Online]. Available: https://unfccc.int/sites/default/files/english_paris_agreement.pdf
- [2] P. J. Menck, J. Heitzig, N. Marwan, and J. Kurths, “How basin stability complements the linear-stability paradigm,” *Nature Physics*, vol. 9, no. 2, pp. 89–92, Feb. 2013, number: 2 Publisher: Nature Publishing Group. [Online]. Available: <https://www.nature.com/articles/nphys2516>
- [3] Z. Liu and Z. Zhang, “Quantifying transient stability of generators by basin stability and Kuramoto-like models,” in *2017 North American Power Symposium (NAPS)*, Sep. 2017, pp. 1–6.
- [4] Z. Liu, X. He, Z. Ding, and Z. Zhang, “A Basin Stability Based Metric for Ranking the Transient Stability of Generators,” *IEEE Transactions on Industrial Informatics*, vol. 15, no. 3, pp. 1450–1459, Mar. 2019, conference Name: IEEE Transactions on Industrial Informatics.

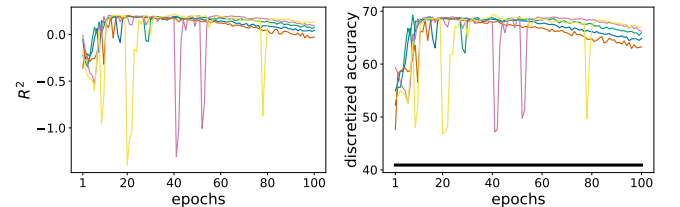


Fig. 13. Training results for dataset100 using ResNet34 and two channel setup. The R^2 -score is shown on the left and the test discretized accuracy on the right. Different colors show different initializations and the vertical line for the discretized accuracy is based on a toy model that always predicts *SNBS*. All evaluations are purely based on the test dataset.

- [5] P. J. Menck, J. Heitzig, J. Kurths, and H. Joachim Schellnhuber, "How dead ends undermine power grid stability," *Nature Communications*, vol. 5, no. 1, p. 3969, Jun. 2014, number: 1 Publisher: Nature Publishing Group. [Online]. Available: <https://www.nature.com/articles/ncomms4969>
- [6] P. Schultz, J. Heitzig, and J. Kurths, "Detours around basin stability in power networks," *New Journal of Physics*, vol. 16, no. 12, p. 125001, Dec. 2014. [Online]. Available: <https://iopscience.iop.org/article/10.1088/1367-2630/16/12/125001>
- [7] H. Kim, S. H. Lee, and P. Holme, "Community consistency determines the stability transition window of power-grid nodes," *New Journal of Physics*, vol. 17, no. 11, p. 113005, Oct. 2015, publisher: IOP Publishing. [Online]. Available: <https://doi.org/10.1088/1367-2630/17/11/113005>
- [8] —, "Building blocks of the basin stability of power grids," *Physical Review E*, vol. 93, no. 6, p. 062318, Jun. 2016, publisher: American Physical Society. [Online]. Available: <https://link.aps.org/doi/10.1103/PhysRevE.93.062318>
- [9] J. Nitzbon, P. Schultz, J. Heitzig, J. Kurths, and F. Hellmann, "Deciphering the imprint of topology on nonlinear dynamical network stability," *New Journal of Physics*, vol. 19, no. 3, p. 033029, Mar. 2017, publisher: IOP Publishing. [Online]. Available: <https://doi.org/10.1088/1367-2630/aa6321>
- [10] H. Kim, S. H. Lee, J. Davidsen, and S.-W. Son, "Multistability and variations in basin of attraction in power-grid systems," *New Journal of Physics*, vol. 20, no. 11, p. 113006, Nov. 2018, publisher: IOP Publishing. [Online]. Available: <https://doi.org/10.1088/1367-2630/aae8eb>
- [11] H. Kim, M. J. Lee, S. H. Lee, and S.-W. Son, "On structural and dynamical factors determining the integrated basin instability of power-grid nodes," *Chaos: An Interdisciplinary Journal of Nonlinear Science*, vol. 29, no. 10, p. 103132, Oct. 2019, publisher: American Institute of Physics. [Online]. Available: <https://aip.scitation.org/doi/abs/10.1063/1.5115532>
- [12] P. Schultz, F. Hellmann, K. N. Webster, and J. Kurths, "Bounding the first exit from the basin: Independence times and finite-time basin stability," *Chaos: An Interdisciplinary Journal of Nonlinear Science*, vol. 28, no. 4, p. 043102, Apr. 2018, publisher: American Institute of Physics. [Online]. Available: <https://aip.scitation.org/doi/10.1063/1.5013127>
- [13] P. Ji, W. Lu, and J. Kurths, "Stochastic basin stability in complex networks," *EPL (Europhysics Letters)*, vol. 122, no. 4, p. 40003, Jun. 2018, publisher: IOP Publishing. [Online]. Available: <https://doi.org/10.1209/0295-5075/122/40003>
- [14] M. Lindner and F. Hellmann, "Stochastic basins of attraction and generalized committor functions," *Physical Review E*, vol. 100, no. 2, p. 022124, Aug. 2019, publisher: American Physical Society. [Online]. Available: <https://link.aps.org/doi/10.1103/PhysRevE.100.022124>
- [15] F. Hellmann, P. Schultz, P. Jaros, R. Levchenko, T. Kapitaniak, J. Kurths, and Y. Maistrenko, "Network-induced multistability through lossy coupling and exotic solitary states," *Nature Communications*, vol. 11, no. 1, p. 592, Jan. 2020, number: 1 Publisher: Nature Publishing Group. [Online]. Available: <https://www.nature.com/articles/s41467-020-14417-7>
- [16] M. F. Wolff, P. G. Lind, and P. Maass, "Power grid stability under perturbation of single nodes: Effects of heterogeneity and internal nodes," *Chaos: An Interdisciplinary Journal of Nonlinear Science*, vol. 28, no. 10, p. 103120, Oct. 2018, publisher: American Institute of Physics. [Online]. Available: <https://aip.scitation.org/doi/10.1063/1.5040689>
- [17] P. Avelar, H. Lemos, M. Prates, and L. Lamb, "Multitask Learning on Graph Neural Networks: Learning Multiple Graph Centrality Measures with a Unified Network," in *Artificial Neural Networks and Machine Learning – ICANN 2019: Workshop and Special Sessions*, ser. Lecture Notes in Computer Science, I. V. Tetko, V. Kůrková, P. Karpov, and F. Theis, Eds. Cham: Springer International Publishing, 2019, pp. 701–715.
- [18] S. K. Maurya, X. Liu, and T. Murata, "Fast Approximations of Betweenness Centrality with Graph Neural Networks," in *Proceedings of the 28th ACM International Conference on Information and Knowledge Management*, ser. CIKM '19. New York, NY, USA: Association for Computing Machinery, Nov. 2019, pp. 2149–2152. [Online]. Available: <https://doi.org/10.1145/3357384.3358080>
- [19] C. Nauck, I. Isenhardt, H. Zhang, F. Hellmann, and P. Ennen, "Prediction of power grid vulnerabilities using machine learning," Master's thesis, Masterarbeit, Rheinisch-Westfälische Technische Hochschule Aachen, 2020, 2020, number: RWTH-2021-00351. [Online]. Available: <https://publications.rwth-aachen.de/record/810053>
- [20] B. Donon, B. Donnot, I. Guyon, and A. Marot, "Graph Neural Solver for Power Systems," in *Proceedings of the International Joint Conference on Neural Networks*, vol. 2019-July. Institute of Electrical and Electronics Engineers Inc., Jul. 2019.
- [21] C. Kim, K. Kim, P. Balaprakash, and M. Animescu, "Graph Convolutional Neural Networks for Optimal Load Shedding under Line Contingency," *Proceedings in IEEE Power Engineering Society General Meeting (to appear, preprint)*, 2019. [Online]. Available: <https://kibaekkim.github.io/papers/PES-GCN-preprint.pdf>
- [22] V. Bolz, J. Rueß, and A. Zell, "Power Flow Approximation Based on Graph Convolutional Networks," in *2019 18th IEEE International Conference On Machine Learning And Applications (ICMLA)*, Dec. 2019, pp. 1679–1686.
- [23] N. Retière, D. T. Ha, and J.-G. Caputo, "Spectral Graph Analysis of the Geometry of Power Flows in Transmission Networks," *IEEE Systems Journal*, vol. 14, no. 2, pp. 2736–2747, Jun. 2020, conference Name: IEEE Systems Journal.
- [24] D. Wang, K. Zheng, Q. Chen, G. Luo, and X. Zhang, "Probabilistic Power Flow Solution with Graph Convolutional Network," in *2020 IEEE PES Innovative Smart Grid Technologies Europe (ISGT-Europe)*, Oct. 2020, pp. 650–654.
- [25] D. Owerko, F. Gama, and A. Ribeiro, "Optimal Power Flow Using Graph Neural Networks," in *ICASSP 2020 - 2020 IEEE International Conference on Acoustics, Speech and Signal Processing (ICASSP)*, May 2020, pp. 5930–5934, iSSN: 2379-190X.
- [26] F. Gama, E. Tolstaya, and A. Ribeiro, "Graph Neural Networks for Decentralized Controllers," Mar. 2020, _eprint: 2003.10280. [Online]. Available: <http://arxiv.org/abs/2003.10280>
- [27] G. S. Misyris, A. Venzke, and S. Chatzivasileiadis, "Physics-Informed Neural Networks for Power Systems," in *2020 IEEE Power Energy Society General Meeting (PESGM)*, Aug. 2020, pp. 1–5, iSSN: 1944-9933.
- [28] Y. Liu, N. Zhang, D. Wu, A. Botterud, R. Yao, and C. Kang, "Searching for Critical Power System Cascading Failures with Graph Convolutional Network," *IEEE Transactions on Control of Network Systems*, pp. 1–1, 2021, conference Name: IEEE Transactions on Control of Network Systems.
- [29] Y. Che and C. Cheng, "Active learning and relevance vector machine in efficient estimate of basin stability for large-scale dynamic networks," *Chaos: An Interdisciplinary Journal of Nonlinear Science*, vol. 31, no. 5, p. 053129, May 2021, publisher: American Institute of Physics. [Online]. Available: <https://aip.scitation.org/doi/abs/10.1063/5.0044899>
- [30] S.-G. Yang, B. J. Kim, S.-W. Son, and H. Kim, "Power-grid stability predictions using transferable machine learning," *arXiv:2105.07562 [physics]*, May 2021, arXiv: 2105.07562. [Online]. Available: <http://arxiv.org/abs/2105.07562>
- [31] L. C. Freeman, "A Set of Measures of Centrality Based on Betweenness," *Sociometry*, 1977.
- [32] P. Schultz, J. Heitzig, and J. Kurths, "A random growth model for power grids and other spatially embedded infrastructure networks," *The European Physical Journal Special Topics*, vol. 223, no. 12, pp. 2593–2610, Oct. 2014. [Online]. Available: <https://doi.org/10.1140/epjst/e2014-02279-6>
- [33] P. Schultz, *luap-pik/SyntheticNetworks*, 2020. [Online]. Available: <https://github.com/luap-pik/SyntheticNetworks>
- [34] G. Filatella, A. H. Nielsen, and N. F. Pedersen, "Analysis of a power grid using a Kuramoto-like model," *The European Physical Journal B*, vol. 61, no. 4, pp. 485–491, Feb. 2008. [Online]. Available: <https://doi.org/10.1140/epjb/e2008-00098-8>
- [35] Y. Kuramoto, "Self-entrainment of a population of coupled non-linear oscillators," in *International Symposium on Mathematical Problems in Theoretical Physics*, 2005.
- [36] F. A. Rodrigues, T. K. D. Peron, P. Ji, and J. Kurths, "The Kuramoto model in complex networks," *Physics Reports*, vol. 610, pp. 1–98, Jan. 2016. [Online]. Available: <https://www.sciencedirect.com/science/article/pii/S0370157315004408>
- [37] M. Gelbrecht, J. Kurths, and F. Hellmann, "Monte Carlo basin bifurcation analysis," *New Journal of Physics*, vol. 22, no. 3, p. 033032, Mar. 2020, publisher: IOP Publishing. [Online]. Available: <https://doi.org/10.1088/1367-2630/ab7a05>
- [38] L. Halekotte, A. Vanselow, and U. Feudel, "Transient chaos enforces uncertainty in the British power grid," *Journal of Physics: Complexity*, vol. 2, no. 3, p. 035015, Jul. 2021, publisher: IOP Publishing. [Online]. Available: <https://doi.org/10.1088/2632-072x/ac080f>
- [39] S. Wallis, "Binomial Confidence Intervals and Contingency Tests: Mathematical Fundamentals and the Evaluation of Alternative Methods," *Journal of Quantitative Linguistics*, vol. 20,

- no. 3, pp. 178–208, Aug. 2013, publisher: Routledge _eprint: <https://doi.org/10.1080/09296174.2013.799918>. [Online]. Available: <https://doi.org/10.1080/09296174.2013.799918>
- [40] J. You, Z. Ying, and J. Leskovec, “Design Space for Graph Neural Networks,” in *Advances in Neural Information Processing Systems*, vol. 33, Curran Associates, Inc., 2020, pp. 17 009–17 021. [Online]. Available: <https://proceedings.neurips.cc/paper/2020/hash/c5c3d4fe6b2cc463c7d7ecba17cc9de7-Abstract.html>
- [41] S. Ioffe and C. Szegedy, “Batch normalization: Accelerating deep network training by reducing internal covariate shift,” in *32nd International Conference on Machine Learning, ICML 2015*, 2015, _eprint: 1502.03167.
- [42] Nitish Srivastava, Geoffrey Hinton, Alex Krizhevsky, Ilya Sutskever, and Ruslan Salakhutdinov, “Dropout: A Simple Way to Prevent Neural Networks from Overfitting,” *Journal of Machine Learning Research*, 2014, iSBN: 1532-4435 _eprint: 1102.4807.
- [43] D. K. Hammond, P. Vandergheynst, and R. Gribonval, “Wavelets on graphs via spectral graph theory,” *Applied and Computational Harmonic Analysis*, vol. 30, no. 2, pp. 129–150, Mar. 2011. [Online]. Available: <https://www.sciencedirect.com/science/article/pii/S1063520310000552>
- [44] T. N. Kipf and M. Welling, “Semi-Supervised Classification with Graph Convolutional Networks,” *arXiv:1609.02907 [cs, stat]*, Feb. 2017, arXiv: 1609.02907. [Online]. Available: <http://arxiv.org/abs/1609.02907>
- [45] F. Wu, T. Zhang, A. H. de Souza, C. Fifty, T. Yu, and K. Q. Weinberger, “Simplifying Graph Convolutional Networks,” Feb. 2019, _eprint: 1902.07153. [Online]. Available: <http://arxiv.org/abs/1902.07153>
- [46] J. Du, S. Zhang, G. Wu, J. M. F. Moura, and S. Kar, “Topology Adaptive Graph Convolutional Networks,” Oct. 2017, _eprint: 1710.10370. [Online]. Available: <http://arxiv.org/abs/1710.10370>
- [47] F. M. Bianchi, D. Grattarola, L. Livi, and C. Alippi, “Graph Neural Networks with Convolutional ARMA Filters,” *IEEE Transactions on Pattern Analysis and Machine Intelligence*, pp. 1–1, 2021, conference Name: IEEE Transactions on Pattern Analysis and Machine Intelligence.
- [48] A. Paszke, S. Gross, F. Massa, A. Lerer, J. Bradbury, G. Chanan, T. Killeen, Z. Lin, N. Gimelshein, L. Antiga, A. Desmaison, A. Kopf, E. Yang, Z. DeVito, M. Raison, A. Tejani, S. Chilamkurthy, B. Steiner, L. Fang, J. Bai, and S. Chintala, “PyTorch: An Imperative Style, High-Performance Deep Learning Library,” in *Advances in Neural Information Processing Systems 32*, H. Wallach, H. Larochelle, A. Beygelzimer, F. d. Alché-Buc, E. Fox, and R. Garnett, Eds. Curran Associates, Inc., 2019, pp. 8024–8035. [Online]. Available: <http://papers.neurips.cc/paper/9015-pytorch-an-imperative-style-high-performance-deep-learning-library.pdf>
- [49] M. Fey and J. E. Lenssen, “FAST GRAPH REPRESENTATION LEARNING WITH PYTORCH GEOMETRIC,” p. 9, 2019. [Online]. Available: <http://arxiv.org/abs/1903.02428>
- [50] J. Bezanson, A. Edelman, S. Karpinski, and V. B. Shah, “Julia: A fresh approach to numerical computing,” *SIAM Review*, 2017, _eprint: 1411.1607.
- [51] C. Rackauckas and Q. Nie, “DifferentialEquations.jl – A Performant and Feature-Rich Ecosystem for Solving Differential Equations in Julia,” *Journal of Open Research Software*, 2017.
- [52] M. Lindner, L. Lincoln, F. Drauschke, J. M. Koulén, H. Würfel, A. Plietzsch, and F. Hellmann, “NetworkDynamics.jl—Composing and simulating complex networks in Julia,” *Chaos: An Interdisciplinary Journal of Nonlinear Science*, vol. 31, no. 6, p. 063133, Jun. 2021, publisher: American Institute of Physics. [Online]. Available: <https://aip.scitation.org/doi/10.1063/5.0051387>
- [53] A. Plietzsch, R. Kogler, S. Auer, J. Merino, A. Gil-de Muro, J. Liße, C. Vogel, and F. Hellmann, “PowerDynamics.jl – An experimentally validated open-source package for the dynamical analysis of power grids,” *arXiv:2101.02103 [cs, eess]*, Jan. 2021, arXiv: 2101.02103. [Online]. Available: <http://arxiv.org/abs/2101.02103>
- [54] M. E. J. Newman, “A measure of betweenness centrality based on random walks,” *Social Networks*, vol. 27, no. 1, pp. 39–54, Jan. 2005. [Online]. Available: <https://www.sciencedirect.com/science/article/pii/S0378873304000681>
- [55] K. He, X. Zhang, S. Ren, and J. Sun, “Deep residual learning for image recognition,” in *Proceedings of the IEEE Computer Society Conference on Computer Vision and Pattern Recognition*, 2016, iSSN: 10636919 _eprint: 1512.03385.